Title

Thermo-Mechanical Level-Set Topology Optimization of an eVTOL Battery Pack

Authors

Guibert, Alexandre T

Bookwala, Murtaza

Cronk, Ashley

et al.

Publication Date

2024-01-08

DOI

10.2514/6.2024-2362

AIAA SciTech Forum
8-12 January 2024, Orlando, FL
AIAA SCITECH 2024 Forum
10.2514/6.2024-2362

Thermo-Mechanical Level-Set Topology Optimization of an eVTOL Battery Pack

Alexandre T. R. Guibert[1], Murtaza Bookwala[1], Ashley Cronk[2], Ying Shirley Meng[3,4] and H. Alicia Kim[1,2*]

[1]Structural Engineering Department, University of California San Diego.
[2]Materials Science and Engineering Department, University of California San Diego.
[3]NanoEngineering Department, University of California San Diego.
[4]Pritzker School of Molecular Engineering, The University of Chicago.

*Corresponding author(s). E-mail(s): alicia@ucsd.edu ;
Contributing authors: aguibert@ucsd.edu; mbookwala@ucsd.edu; acronk@eng.ucsd.edu; shirleymeng@uchicago.edu;

Abstract

Electric Vertical Take-Off and Landing (eVTOL) vehicles are considered a promising solution to alleviate traffic congestion and provide an alternative to traditional individual transportation. The design and performance of eVTOL battery packs play a critical role in the development of this mode of transportation. In this paper, we propose a methodology to topologically optimize an eVTOL battery pack using the level-set topology optimization method while considering multi-physics loading conditions. The objective is to obtain a thermally and structurally efficient lightweight structure. At the system level, a linear elastic beam model is developed to model the boom where the battery pack is located and obtain the mechanical load carried by the battery pack due to its placement in the vehicle. At the battery scale, a physics-based electrochemical model is applied to predict the maximum heat generation of the batteries due to the power requirements from a given mission profile. The mechanical load from the system

scale and the thermal load from the battery scale are considered inputs for the battery pack thermo-mechanical model used for optimization.

Keywords: eVTOL, multiphysics optimization, level-set topology optimization

1 Introduction

With concerns over climate change and the need to reduce carbon emissions, electric vehicles (EV) gained significant attention as a viable alternative to traditional gasoline-powered vehicles in the last two decades [1]. The development of advanced battery technology and charging infrastructure has contributed to the undergoing market growth of EVs in the automotive industry. Recently there has been increasing efforts to apply the same principle to the aerospace sector.

One of the challenges for the development of eVTOL vehicles is the energy requirements and power density of the batteries [2]. Additionally, the battery pack in an eVTOL vehicle is subjected to various loads during flights. The external loadings arise from physics at different scales, i.e., the aircraft scale during the flight due to a given maneuver, to the molecular scale due to the electrochemical reactions in the cells. In this work, we propose a methodology to account for multiscale loading via topology optimization of an eVTOL battery pack. The objective is to obtain a lightweight thermally and structurally efficient design.

The workflow and the mission profile are first discussed in Section 2. The battery placement considered for this work is presented in Section 3 before introducing the numerical models of the aircraft boom, battery pack, and batteries in Section 4. The level-set topology optimization scheme is discussed in Section 5. Finally, the example battery pack designs are optimized in Section 6.

2 Workflow and mission profile

First, the power profile from the specified mission is taken from [3] with a cruise segment of 400 s. A power of 43.2 W is used for the landing and takeoff segments, and 16 W is used for the cruise segment. The power requirements are then passed to an electrochemical model which serves two purposes: first, to estimate the electrochemical response and second to predict the volumetric heat generation from the batteries. The load from the rotors is fed into a linear elastic beam model of the boom where the cells are placed to determine the mechanical loading on the pack. The heat generation and the mechanical loading are inputs for the coupled thermo-mechanical finite element model of the battery pack. A heat conduction equation is solved to determine the temperature distribution in the pack and this temperature field is then used

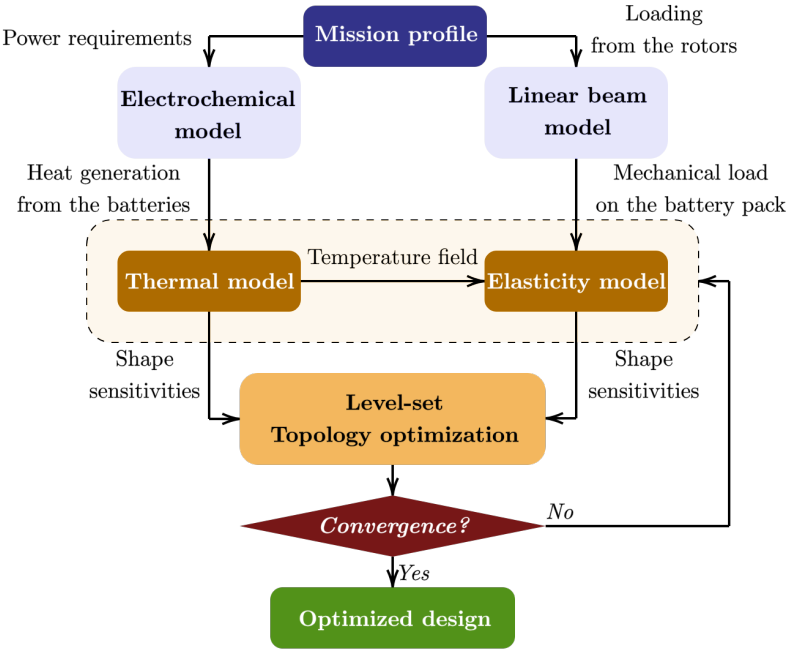

Fig. 1: eVTOL battery pack optimization workflow

to compute the thermal strain. The battery pack is modeled assuming linear elasticity. From the coupled thermo-mechanical model, shape sensitivities are computed using the adjoint method and utilized by a gradient-based topology optimization algorithm to optimize the design of the battery pack in the volume available in a boom. The overall workflow is presented schematically in Fig. 1.

3 Battery pack placement

Electric aircraft require a large number of batteries stored in the vehicle while maximizing the volume available for payload. Possible locations considered for the batteries are

1. inside the wing where the fuel is stored in traditional aircraft
2. in the booms, i.e., inside the component that connect the rotors to the wing
3. under the floor of the cabin

This work studies storing the battery cells in the booms as they offer good proximity to the electric motors and their placement is shown in Fig. 2.

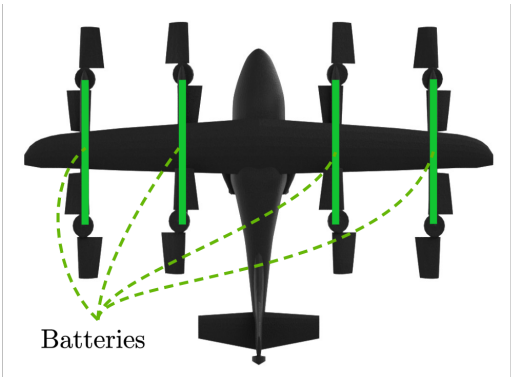

Fig. 2: Schematic of the battery placements in this eVTOL study. The model of the eVTOL is taken from [4]

4 Numerical models

4.1 Linear elastic beam model

A boom is idealized as a beam with point loads at the two extremities due to the rotors. The center part of the boom is attached to the wing and is considered fixed in all degrees of freedom. Timoshenko-Ehrenfest beam theory [5] is assumed and the effective section properties for the beam are computed based on the skin of the boom made out of Aluminum. The second moment of inertia I of the boom should be recomputed as the design evolves. However, as a simplification, it is only computed once without considering the change of the second moment of inertia due to the boom internal structure. Thus, the second moment of inertia is computed as:

$$I = \frac{\pi}{4}(r_{out}^4 - r_{in}^4) \tag{1}$$

where r_{out} and r_{in} are the outer and inner radii of the boom respectively. The shear correction factor κ_{shear} is taken from Cowper [6] as

$$\kappa_{shear} = \frac{2(1+\nu)}{4+3\nu} \tag{2}$$

where ν is the Poisson's ratio. The governing equations for the beam are

$$\frac{d^2}{dx^2}\left(EI\frac{d\theta}{dx}\right) = q(x) \tag{3}$$

$$\frac{dw}{dx} = \theta - \frac{1}{\kappa_{shear}AG}\frac{d}{dx}\left(EI\frac{d\theta}{dx}\right) \tag{4}$$

where A is the cross-sectional area, E is the Young's modulus, G is the shear modulus, and $q(x)$ is a distributed load. The model is solved for the displacement of the mid-surface w and rotation of the normal to the mid-surface of the beam θ. The model is shown schematically in Fig. 3. Due to symmetry, only half the boom will be modeled. It is also worth noting that some space was left available intentionally for wiring and battery management systems.

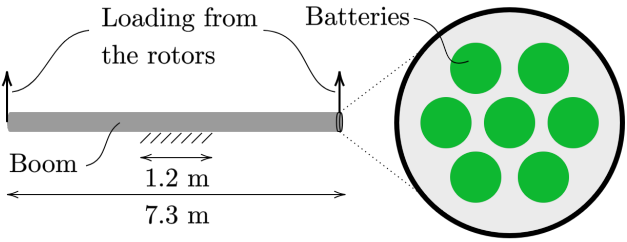

Fig. 3: Schematic of the boom model idealized as the beam and the cells in its cross-section

The shear forces and bending moments calculated from the Timoshenko-Ehrenfest beam theory are used to calculate stresses in the cross-section of the beam. These stresses are then used to calculate the loads on the battery pack for the optimization problem.
The axial stress due to the bending moment is given by:

$$\sigma_{xx} = \frac{Mh}{I} \tag{5}$$

The shear stress due to shear force is written as:

$$\tau_{xy} = \frac{V\mathcal{Q}}{Ib} \tag{6}$$

Here, $\mathcal{Q}$ is the first moment of area, h is the height of a point above the neutral axis of the beam, and b is the breadth of the beam. The axis along the length of the beam is the x-axis, and y is orthogonal to x in the plane of bending.

4.2 Electrochemical model

The Doyle-Fuller-Newman (DFN) model [7, 8] of a lithium-ion battery is chosen as the physics-based electrochemical model to predict the volumetric heat generation rate from the batteries [9]. This model is based on charge conservation, molar conservation, and intercalation kinetics, and is solved using the finite volume method [10]. The model is implemented with the open-source

Python library PyBaMM [11]. It is used the predict the volumetric heat generated by the batteries due to the ohmic heating, electrochemical reactions, and entropic changes. The maximum volumetric heat generation is then considered as an input for the thermo-mechanical finite element model.

4.3 Thermo-mechanical model

The battery pack behavior is modeled assuming a weak coupling between the thermal model and the elasticity model. This is reasonable under the small deformations assumption and the assumption that the displacement field does not have a significant effect on the temperature field. First, the steady-state heat conduction problem is solved for the temperature and the governing equation is

$$\nabla \cdot (\kappa \nabla T) + Q = 0 \tag{7}$$

where κ is the thermal conductivity and T is the temperature. The source term Q is computed from the electrochemical model in Section 4.2. From the heat conduction solution, the temperature field is passed to the linear elasticity model. The governing equation of linear elasticity is,

$$\nabla \cdot \boldsymbol{\sigma}(\boldsymbol{u}) + \boldsymbol{b} = 0 \tag{8}$$

where $\boldsymbol{b}$ is the body force, $\boldsymbol{u}$ is the displacement, and $\boldsymbol{\sigma}$ is the Cauchy stress tensor. The constitutive law considering thermal strain is given as

$$\boldsymbol{\sigma} = \mathbb{C} : (\boldsymbol{\varepsilon} - \varepsilon_T \mathbf{1}) \tag{9}$$

where $\mathbb{C}$ is the elasticity constitutive tensor, $\boldsymbol{\varepsilon}$ is the strain tensor, and ε_T is the thermal strain. The thermo-mechanical model is implemented using the open-source finite element library FEniCSx [12]. For scalability, the model is implemented using distributed memory parallel computing using message passing interface (MPI) [13].

5 Level-set topology optimization

Level-set topology optimization (LSTO) is a gradient-based optimization method [14]. The optimized design Ω is described by an implicit level-set function $\phi(x)$ where x is a point in the design domain $\mathcal{D}$ such that,

$$\begin{cases} \phi(x) \geq 0 \iff x \in \Omega \subset \mathcal{D} \\ \phi(x) = 0 \iff x \in \partial\Omega \\ \phi(x) < 0 \iff x \in \mathcal{D} \setminus \Omega \end{cases} \tag{10}$$

The design is iteratively updated by advecting the zero level-set using the Hamilton-Jacobi equation, so-called the level-set equation,

$$\frac{\partial \phi(x)}{\partial t} + |\nabla \phi(x)| V_n(x) = 0 \tag{11}$$

where t is the pseudo-time and V_n is the normal component of the design velocity computed by solving the associated suboptimization problem at each optimization iteration [15]. The adjoint method is employed to compute the sensitivities of the constraints and objective functions needed for the sub-optimization problem [16]. The LSTO method is implemented using the modularized open-source code ParaLeSTO [17]. More details regarding the modularity of ParaLeSTO can be found in [18, 19].

6 Numerical examples

6.1 Problem setup

The battery selected for this work is the LG Chem 21700M50LT battery and the parameters for the electrochemical models are taken from [20]. We assume a container made of the same Aluminum as the boom and the properties are given in Table 1. The section of the boom near the wing, where

Table 1: Properties for the thermo-mechanical analysis

Property	Aluminum	Cell
Thermal conductivity κ [W/m.K]	220.0	1.25
Young's modulus E [GPa]	68.0	1.5
Poisson's ratio ν [-]	0.32	0.2
Thermal expansion α [K^{-1}]	$21x10^{-6}$	$10x10^{-6}$

the bending moment is maximum, is considered for optimization. However, the methodology is applicable to the entire boom given appropriate computational resources. The dimensions of the design domain are given in Fig. 4. The boundary conditions are functions of the input models, i.e., the beam and electrochemical models, and will be discussed in the next Section. The design domain is discretized with 120x101x120 hexahedra finite elements resulting in 5,973,528 degrees of freedom.

6.2 Beam and electrochemical models results

The electrochemical and beam models serve as inputs for the thermo-mechanical battery pack analysis. Thus, we will first discuss these results starting with the electrochemical model. The terminal voltage and volumetric heat generation obtained with the selected power profile are presented in Fig. 5. We observed that the voltage cut-off was not reached and that the battery was able to complete the power profile. In addition, the maximum heat generation is 179.41 $kW.m^{-3}$. This value will be used for the thermo-mechanical analysis assuming a uniform distribution in each battery.

A disk loading of 222 $N.m^{-2}$ with rotor disk area of 7.45 m^2 is used for this work [21]. Thus, a load of 1653.9 N is applied as a boundary condition for the

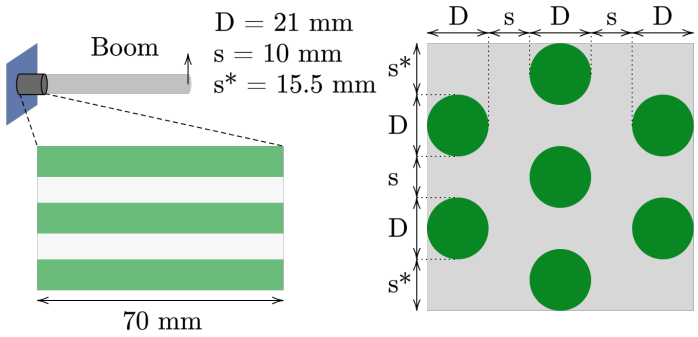

Fig. 4: Design domain for optimization, in grey, and batteries as non-design domains, in green

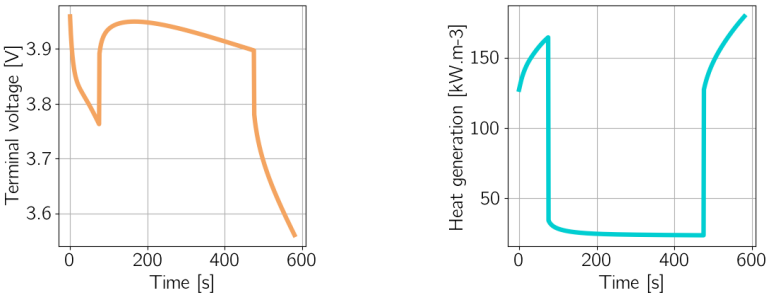

(a) Voltage profile

(b) Heat generation

Fig. 5: LG Chem 21700M50LT Battery response to power profile

boom model. The length of the beam is 3.05 m from Fig. 3. The inner and outer radii for the boom are taken as 58.7 mm and 63.7 mm respectively. The inner radius is taken such that the design domain is inscribed in the boom which also leaves room to wiring and battery management systems. The outer radius is such that the aluminum skin has a thickness of 5 mm. The beam model is discretized with 1000 finite elements and the results are presented in Fig. 6

It is worth noting that for a simple beam such as the one present here, analytical solutions exist and were used to validate the numerical model. For instance, the maximum deflection d_{max} of a cantilever beam subjected to a concentrated load P at the end is $PI^3/3EI = 0.0638$ m. The tip deflection using the finite element model is 0.0640 m, resulting in a relative error of 0.3 %. Even though the exact solutions exist for simple beams, a general model is desirable to be expandable in future work. The shear force and bending moment are then used to compute the mechanical boundary conditions applied to the

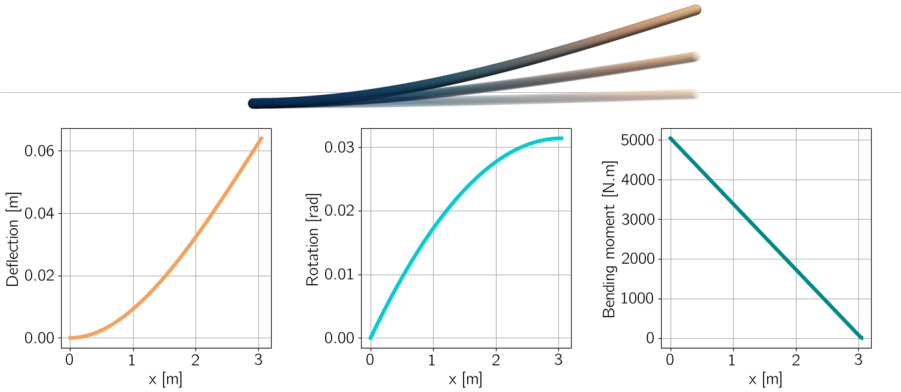

Fig. 6: Beam response to rotor load: deflection (left), rotation (center), and bending moment (right)

battery pack as described in Section 4.1. The mechanical loads are applied as traction loads on four arbitrary locations on one face. The displacements in all directions on the same four locations on the opposite face are fixed. The sides of the battery pack are considered heat sinks. The thermal and mechanical boundary conditions for the battery pack are shown in Fig. 7

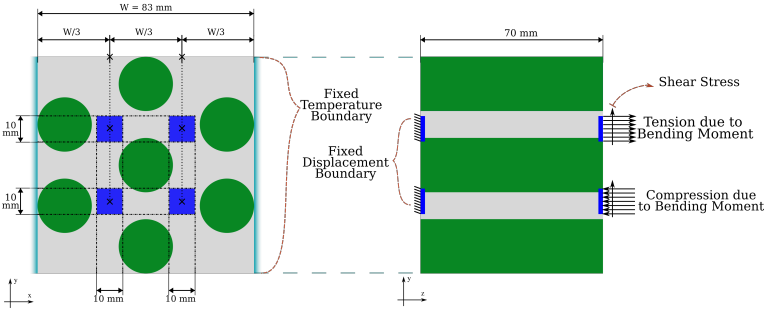

Fig. 7: Mechanical and thermal boundary conditions for the battery pack optimization problem

6.3 Battery pack thermo-mechanical optimization

The optimization problem consists of the minimization of the weighted sum of thermal compliance C_T and structural compliance C_S subjected to a volume constraint such that the optimization problem reads

$$\begin{aligned} \min_{\Omega} \quad & kC_S/C_S^0 + (1-k)C_T/C_T^0 \\ \text{subject to} \quad & \text{Vol}(\Omega) \leq \xi \, \text{Vol}(\mathcal{D}) \end{aligned} \tag{12}$$

$$\mathcal{R} = 0$$

where k controls the weight given to the structural compliance and thermal compliance and $\square^0$ indicates an initial value. The prescribed volume fraction is ξ and is set to be 45 %. $\mathcal{R}$ is the residuals of the system being solved. The thermal compliance and structural compliance are defined as

$$C_S = \mathbf{f}_M^\top \mathbf{u}^h \tag{13}$$

$$C_T = \mathbf{f}_T^\top \mathbf{T}^h \tag{14}$$

where $\mathbf{f}_M$ and $\mathbf{f}_T$ are the vectors of mechanical and thermal loads, respectively. The vector of nodal displacements is $\mathbf{u}^h$ and $\mathbf{T}^h$ is the vector of nodal temperatures. The optimization history of C_S and C_T for different values of k are presented in Fig. 8. The optimized designs for 4 selected cases are shown in

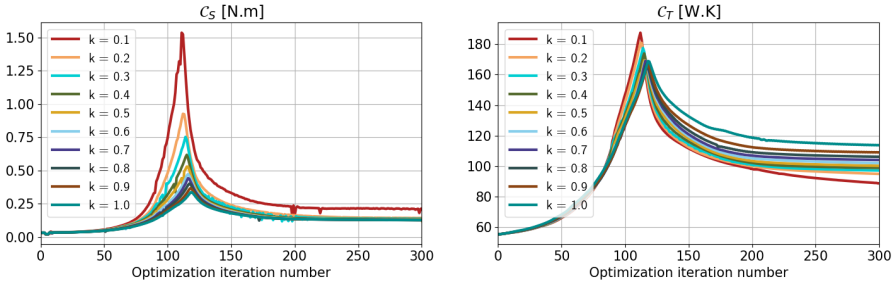

Fig. 8: Optimization history of the structural compliance (left) and thermal compliance (right)

Fig. 9. We can see that with lower values of k, there exist more direct conduction paths from the heat source, i.e., the batteries, to the heat sinks, i.e., the side surfaces. As k is increased, the conduction paths transition to truss-like structures.

The temperature distribution of 4 selected cases and the displacement magnitude of the same 4 cases are shown in Fig. 10 and Fig. 11. In Fig. 10 we can observe that the maximum temperature increases with an increase in the weight given to structural compliance. Temperature distribution also gets more uniform as we increase the weight given to C_T. Analogous results are observed when considering displacement in the pack. From Fig. 11 the inverse relationship between the weight given to minimizing C_S and the maximum displacement is clear.

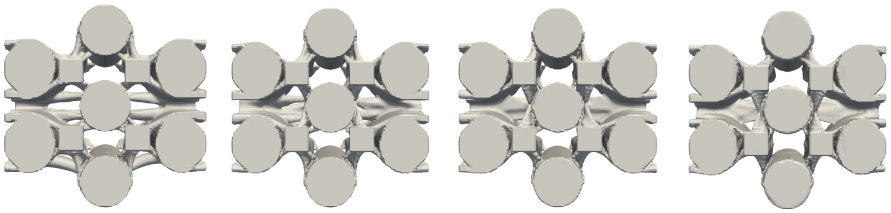

(a) $k = 0.2$ (b) $k = 0.4$ (c) $k = 0.8$ (d) $k = 1.0$

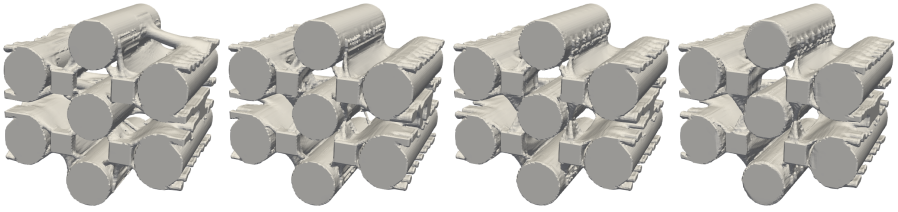

(e) $k = 0.2$ (f) $k = 0.4$ (g) $k = 0.8$ (h) $k = 1.0$

Fig. 9: Optimized battery packs for four selected cases

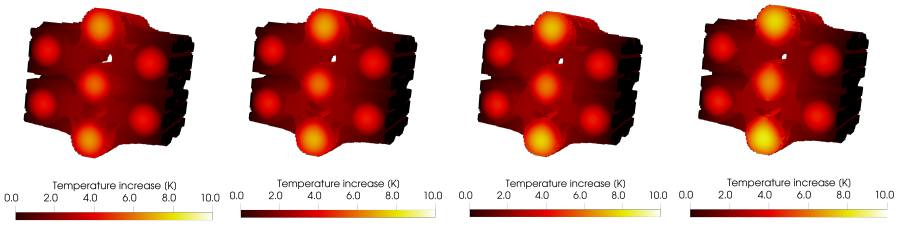

(a) $k = 0.2$ (b) $k = 0.4$ (c) $k = 0.8$ (d) $k = 1.0$

Fig. 10: Temperature distribution [in K] of optimized battery packs for selected cases

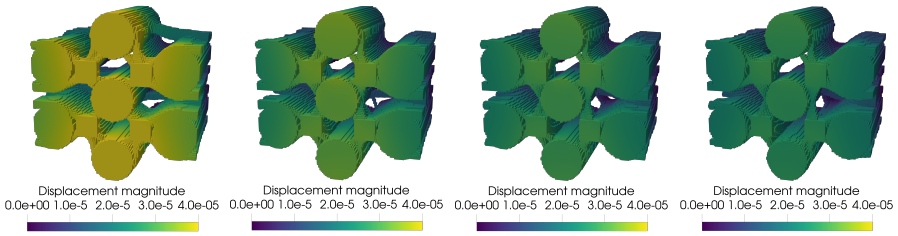

(a) $k = 0.2$ (b) $k = 0.4$ (c) $k = 0.8$ (d) $k = 1.0$

Fig. 11: Displacement magnitude [in m] of optimized battery packs for selected cases

7 Conclusions

This study focuses on enhancing the performance of an electric Vertical Takeoff and Landing (eVTOL) aircraft's battery pack by utilizing level-set topology optimization. A physics-based electrochemical model, the Doyle-Fuller-Newman model, was used to predict the heat generated by the batteries. To estimate the mechanical loads on the battery pack, a Timoshenko-Ehrenfest beam model, which represents the structural elements of the eVTOL where the batteries will be placed, is employed. The mechanical and thermal loads, derived from the electrochemical and beam models, are incorporated as boundary conditions in a finite element thermo-mechanical model of the battery pack.

The objective is to optimize the battery pack taking into account both thermal and structural factors. A weighted sum of thermal compliance and structural compliance, normalized by their initial values, is used as an objective function for the optimization process. We demonstrate that topology optimization can be used to design battery packs while considering external loadings from different scales. We present the optimization results for various weights, along with temperature distribution and displacement magnitude for four specific scenarios.

Our findings reveal that there is a trade-off between maximum displacement and maximum temperature, and this trade-off can be controlled by adjusting the weight assigned to each objective. Importantly, we note that as the weight for structural compliance increases, there is an increase in temperature variation among individual battery cells. Ideally, we want to minimize temperature differences between cells to prevent variations in degradation rates within the same battery pack. To address this, future work will incorporate temperature variance as part of the optimization process. Furthermore, we plan to expand our research to include temperature and stress constraints in the optimization formulation.

Acknowledgments

The authors acknowledge the support from NASA under award No. 80NSSC21M0070.

References

[1] Sanguesa, J.A., Torres-Sanz, V., Garrido, P., Martinez, F.J., Marquez-Barja, J.M.: A review on electric vehicles: Technologies and challenges. Smart Cities **4**(1), 372–404 (2021)

[2] Wheeler, P., Bozhko, S.: The more electric aircraft: Technology and challenges. IEEE Electrification Magazine **2**(4), 6–12 (2014)

[3] Bills, A., Sripad, S., Fredericks, L., Guttenberg, M., Charles, D., Frank, E., Viswanathan, V.: A battery dataset for electric vertical takeoff and landing aircraft. Scientific Data **10**(1), 344 (2023)

[4] Center, N.L.R.: NASA Urban Air Mobility (UAM) Reference Vehicles. https://sacd.larc.nasa.gov/uam-refs/ (2023)

[5] Elishakoff, I.: Handbook on timoshenko-ehrenfest beam and uflyand-mindlin plate theories (2020)

[6] Cowper, G.: The shear coefficient in timoshenko's beam theory. Journal of applied mechanics **33**(2), 335–340 (1966)

[7] Newman, J.S., Tobias, C.W.: Theoretical analysis of current distribution in porous electrodes. Journal of The Electrochemical Society **109**(12), 1183 (1962). https://doi.org/10.1149/1.2425269

[8] Doyle, M., Fuller, T.F., Newman, J.: Modeling of galvanostatic charge and discharge of the lithium/polymer/insertion cell. Journal of The Electrochemical Society **140**(6), 1526–1533 (1993). https://doi.org/10.1149/1.2221597

[9] Timms, R., Marquis, S.G., Sulzer, V., Please, C.P., Chapman, S.J.: Asymptotic reduction of a lithium-ion pouch cell model. SIAM Journal on Applied Mathematics **81**(3), 765–788 (2021)

[10] Eymard, R., Gallouët, T., Herbin, R.: Finite volume methods. Handbook of numerical analysis **7**, 713–1018 (2000)

[11] Sulzer, V., Marquis, S.G., Timms, R., Robinson, M., Chapman, S.J.: Python Battery Mathematical Modelling (PyBaMM). Journal of Open Research Software **9**(1), 14 (2021). https://doi.org/10.5334/jors.309

[12] Alnæs, M., Blechta, J., Hake, J., Johansson, A., Kehlet, B., Logg, A., Richardson, C., Ring, J., Rognes, M.E., Wells, G.N.: The fenics project version 1.5. Archive of Numerical Software **3**(100) (2015)

[13] Gropp, W., Lusk, E., Skjellum, A.: Using MPI: Portable Parallel Programming with the Message-passing Interface vol. 1. MIT press, ??? (1999)

[14] Sivapuram, R., Dunning, P.D., Kim, H.A.: Simultaneous material and structural optimization by multiscale topology optimization. Structural and multidisciplinary optimization **54**, 1267–1281 (2016)

[15] Dunning, P.D., Kim, H.A.: Introducing the sequential linear programming

level-set method for topology optimization. Structural and Multidisciplinary Optimization **51**, 631–643 (2015)

[16] Kambampati, S., Chung, H., Kim, H.A.: A discrete adjoint based level set topology optimization method for stress constraints. Computer Methods in Applied Mechanics and Engineering **377**, 113563 (2021)

[17] Kambampati, S., Jauregui, C.M.: ParaLeSTO. https://doi.org/10.5281/zenodo.7613753. https://doi.org/10.5281/zenodo.7613753

[18] Hyun, J., Jauregui, C., Kim, H.A., Neofytou, A.: On development of an accessible and non-intrusive level-set topology optimization framework via the discrete adjoint method. In: AIAA SCITECH 2022 Forum, p. 2548 (2022)

[19] Guibert, A.T., Hyun, J., Neofytou, A., Kim, H.A.: Implementation of a plug-and-play reusable level-set topology optimization framework via comsol multiphysics. In: AIAA SCITECH 2023 Forum, p. 1675 (2023)

[20] Chen, C.-H., Planella, F.B., O'regan, K., Gastol, D., Widanage, W.D., Kendrick, E.: Development of experimental techniques for parameterization of multi-scale lithium-ion battery models. Journal of The Electrochemical Society **167**(8), 080534 (2020)

[21] Weitsman, D., Greenwood, E.: Parametric study of evtol rotor acoustic design trades. In: AIAA Scitech 2021 Forum, p. 1987 (2021)